Quantification of Peripapillary Sparing and Macular Involvement in Stargardt Disease (STGD1)

Tomas R. Burke,[1] *David W. Rhee,*[2] *R. Theodore Smith,*[1,3] *Stephen H. Tsang,*[1,4] *Rando Allikmets,*[1,4] *Stanley Chang,*[1] *Margot A. Lazow,*[2] *Donald C. Hood,*[1,2] *and Vivienne C. Greenstein*[1]

Purpose. To quantify and compare structure and function across the macula and peripapillary area in Stargardt disease (STGD1).

Methods. Twenty-seven patients (27 eyes) and 12 age-similar controls (12 eyes) were studied. Patients were classified on the basis of full-field electroretinogram (ERG) results. Fundus autofluorescence (FAF) and spectral domain-optical coherence tomography (SD-OCT) horizontal line scans were obtained through the fovea and peripapillary area. The thicknesses of the outer nuclear layer plus outer plexiform layer (ONL+), outer segment (OS), and retinal pigment epithelium (RPE) were measured through the fovea, and peripapillary areas from 1° to 4° temporal to the optic disc edge using a computer-aided, manual segmentation technique. Visual sensitivities in the central 10° were assessed using microperimetry and related to retinal layer thicknesses.

Results. Compared to the central macula, the differences between controls and patients in ONL+, OS, and RPE layer thicknesses were less in the nasal and temporal macula. Relative sparing of the ONL+ and/or OS layers was detected in the nasal (i.e., peripapillary) macula in 8 of 13 patients with extramacular disease on FAF; relative functional sparing was also detected in this subgroup. All 14 patients with disease confined to the central macula, as detected on FAF, showed ONL+ and OS layer thinning in regions of normal RPE thickness.

Conclusions. Relative peripapillary sparing was detected in STGD1 patients with extramacular disease on FAF. Photoreceptor thinning may precede RPE degeneration in STGD1. (*Invest Ophthalmol Vis Sci.* 2011;52:8006–8015) DOI:10.1167/iovs.11-7693

From the Departments of [1]Ophthalmology, [2]Psychology, [3]Biomedical Engineering, and [4]Pathology and Cell Biology, Columbia University, New York, New York.

Supported by The Eye Surgery Fund; National Eye Institute Grants EY-09076, EY-015520, EY-017404, and EY-13435; unrestricted funds from Research to Prevent Blindness; the Foundation Fighting Blindness grants CD0CBT-0807-0425FFB and C-NY05-0705-0312 (Owings Mills, MD); New York State Grant N09G-302; United States Department of Defense Grant TS080017; the Crowley Family Research Fund; the Schneeweiss Stargardt Fund; and unrestricted funds from Research to Prevent Blindness (New York, New York) and The Starr Foundation.

Submitted for publication April 5, 2011; revised July 8, 2011; accepted August 5, 2011.

Disclosure: **T.R. Burke**, None; **D.W. Rhee**, None; **R.T. Smith**, None; **S.H. Tsang**, None; **R. Allikmets**, None; **S. Chang**, None; **M.A. Lazow**, None; **D.C. Hood**, Topcon (C); **V.C. Greenstein**, None

Corresponding author: Tomas R. Burke, Edward S. Harkness Eye Institute, 160 Fort Washington, New York, NY 10032; tomasburke30@gmail.com.

Mutations in the *ABCA4* gene are the known cause of autosomal recessive Stargardt disease (STGD1).[1] The ABCA4 protein is the transporter of vitamin A derivatives in the outer segment disc membranes of photoreceptors. In the absence of functional protein due to mutations in the gene, vitamin A aldehyde forms bis-retinoid adducts that are deposited in retinal pigment epithelial (RPE) cells during the process of disc shedding and phagocytosis.

One of the features of *ABCA4* disease is relative peripapillary sparing, characterized by the absence of flecks and RPE atrophy in the peripapillary region of the retina.[2–5] The presence of either is termed peripapillary atrophy. Recent reports have shown that a small percentage of patients with STGD1 develop peripapillary atrophy.[6,7] We have demonstrated peripapillary atrophy using fundus autofluorescence (FAF) in patients classified as ERG group II or III STGD1.[8] The classification was based on full-field electroretinogram (ERG) results. Patients with a normal scotopic and photopic ERGs are classified as group I).[9] Patients with ERG group II disease have decreased photopic ERGs, whereas patients with ERG group III disease have decreased scotopic and photopic ERGs.[9] In our previous study, 1 of 15 patients in group I, all 7 patients in group II, and 9 of 10 patients in group III demonstrated peripapillary atrophy.[8]

Because of the relative sparing of the peripapillary area in *ABCA4* disease, it has been suggested that this is a region of interest for monitoring the efficacy of treatment in this disease.[2] Therefore detailed structural and functional characterization of this retinal region is of interest. Whereas previous methods of assessing the peripapillary retina have focused on its appearance using en face imaging,[2–5,8] we used spectral-domain optical coherence tomography (SD-OCT) to evaluate the integrity of the outer retinal layers and RPE and microperimetry to assess visual function in this region and across the macula. Both modalities use retinal tracking features to compensate for eye movement during examination, a feature essential in assessing *ABCA4* disease phenotypes with reduced visual acuity and unstable fixation.

Materials and Methods

Subjects

Twenty-seven patients (12 male, 15 female) with a mean age of 32.5 ± 13.9 years (range, 14–59) and 12 age-similar controls with a mean age of 32.7 ± 14.6 years (range, 15–52) were prospectively recruited for the study. There was no significant difference in age at examination between the two groups. In each subject, the eye with the best corrected visual acuity was included. When visual acuities were equal in both eyes, the eye with the lowest refractive error was chosen.

Inclusion criteria were a clinical diagnosis of *ABCA4* retinopathy, confirmed by genotyping, and no significant ocular media opacities. Exclusion criteria were a refractive error greater than ±6 D sphere or

Investigative Ophthalmology & Visual Science, October 2011, Vol. 52, No. 11

±2 D cylinder, intraocular pressure (IOP) > 21 mm Hg, a history or diagnosis of any other significant ocular co-morbidities, poor-quality OCT scans, or unreliable microperimetry. Age at examination was documented for all patients.

All participants were recruited at the Department of Ophthalmology, Columbia University, New York. The study was conducted in accordance with the ethical standards set out in the Declaration of Helsinki and was approved by the institutional review board at Columbia University. Informed consent was obtained from all subjects before enrollment in the study.

Clinical Examination

All subjects underwent a complete ocular examination, including best corrected visual acuity with an Early Treatment Diabetic Retinopathy screening chart 1 (ETDRS Chart 1) with subjective refraction. Slit lamp biomicroscopy was performed after IOP measurement with Goldmann applanation tonometry. Direct and indirect funduscopy was performed after pupil dilation with 1% tropicamide. Phlebotomy was performed for genotyping.

Preferred Retinal Location and Microperimetry

Visual field sensitivities, preferred retinal location (PRL), and fixation stability were evaluated in all subjects by microperimetry (MP-1; Nidek Technologies, Inc., Padova, Italy) after pupil dilation with 1% tropicamide. The nontested eye was occluded throughout the procedure. Patients were asked to maintain fixation on a red cross (2° in diameter) for the duration of the test. The sensitivity of the 68 sampling points in the central 20° visual field was determined with a 10-2 program after 15 minutes of adaptation to the background luminance. White test lights (stimulus size, Goldmann III; duration, 200 ms) were presented on a dim white background (1.27 cd/m^2), with a 4-2 threshold strategy. Total deviation (TD) plots were calculated for each patient by subtracting the sensitivity at a given location from the mean sensitivities of the control subjects at these locations. Fixation stability was defined based on the bivariate contour ellipse area (BCEA).[10] Examples of macular microperimetry are shown in Figure 1.

Coregistration of the visual field results with the en face images was performed using the software provided with the microperimeter (Navis Software, ver. 1.7; Nidek Technologies, Inc.). The en face image, which was acquired simultaneously with the SD-OCT image on a confocal laser scanning ophthalmoscope (Spectralis HRA+OCT; Heidelberg Engineering, Dossenheim, Germany), was imported into the microperimeter and registered with the corresponding visual field result. Importantly, the line indicating the position of the SD-OCT on the en face image was visible during this process, thus indicating which test points were to be correlated to thickness measurements. The distance between each test point was taken as 2°, and so the thicknesses at each test point could be calculated from the data derived from the analysis of the SD-OCT line scan (see below).

Full-Field ERG

Ganzfeld full-field scotopic and photopic ERGs (Diagnosys LLC, Lowell, MA) were recorded from both eyes with DTL electrodes according to the International Society for Clinical Electrophysiology of Vision (ISCEV) standards.[11] The amplitudes and implicit times obtained from each patient were compared to values from age-similar normal controls. Responses with amplitude reductions ≥2 SD from the mean for age-similar controls were considered abnormal, and patients were stratified on the basis of ERG results.[9] The authors considered implicit time delays ≥2 SD to be abnormal also. In this study, patients with ERG group III disease were excluded, as the eccentricity and/or instability of fixation precluded accurate measurement of the macular visual sensitivities.

SD-OCT Examinations

All individuals were scanned with SD-OCT (Spectralis HRA+OCT) using the eye-tracking feature after pupil dilation with 1% tropicamide. A horizontal 9-mm line scan, centered on the fovea with the nasal end of the line scan passing through or within 1° of the disc edge, was obtained as an average of 100 scans. This scan was used to assess retinal layer thicknesses across the macula, as well as for comparison of nasal and temporal macular thicknesses. When the retinal architecture was very abnormal in the central macula, the region with the greatest retinal thinning was deemed the location of the fovea at the time of SD-OCT line scan acquisition and was consistent with measure-

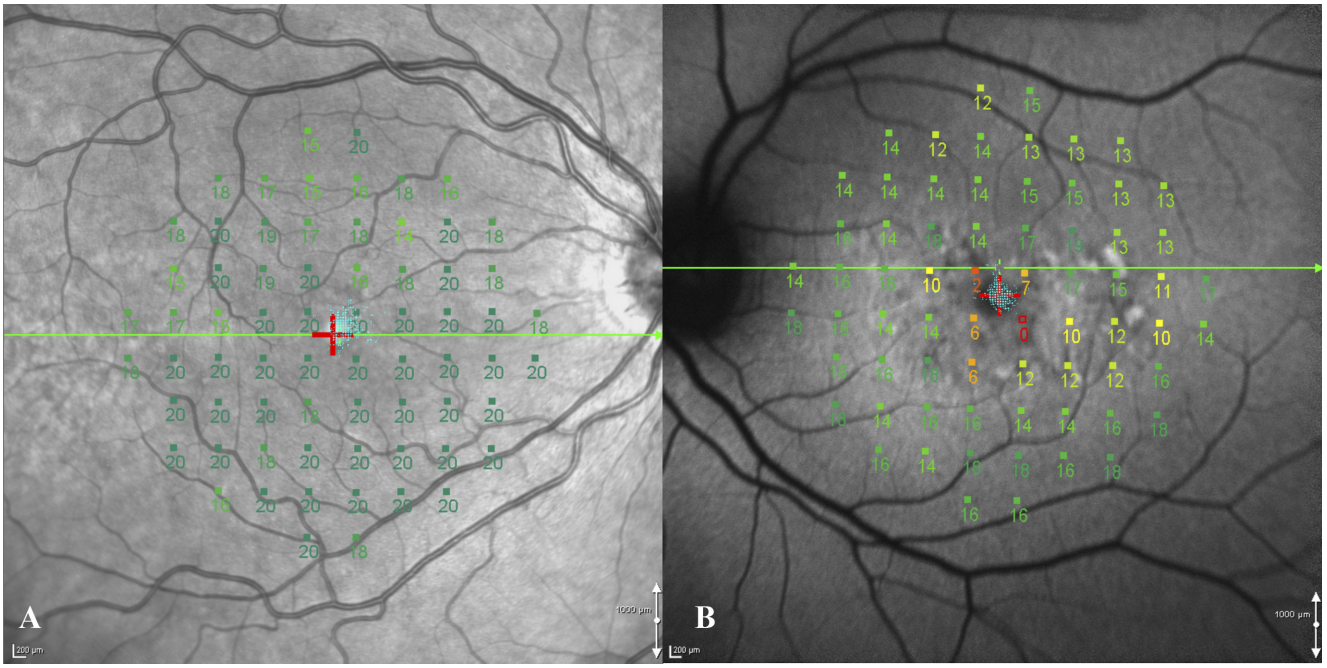

Figure 1. **(A)** Microperimetry results from a control subject registered to the IR image. There was stable fixation. Note the position of the line scan (*green horizontal line* through the fovea). **(B)** Microperimetry results from a patient with stable fixation, registered to an FAF image.

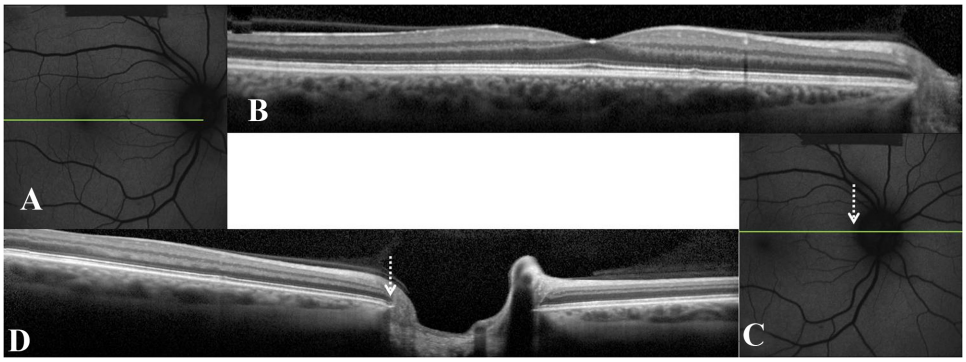

FIGURE 2. FAF (**A**, **C**) and corresponding SD-OCT scans (**B**, **D**) of a control. *Horizontal green line*: the position of the SD-OCT scan. In this case, the horizontal macular line scan (**B**) did not bisect the optic disc. Therefore, a second horizontal SD-OCT line scan which bisected the optic disc was acquired (**D**). *White-dashed arrow*: position of the optic disc edge.

ments available from previous studies documenting the location of the fovea relative to the optic disc in normal subjects.[12,13]

For direct comparison of the peripapillary area from 1° to 4° temporal to the optic disc edge, between patients and controls, only horizontal line scans that bisected the optic disc were used. Where the macular line scan had not bisected the optic disc, another 9-mm horizontal line scan centered on and bisecting the optic disc was acquired for this additional analysis (Fig. 2). The optic disc edge provided a fixed reference point to allow comparison of thicknesses in the peripapillary area between subjects for subanalysis.

Segmentation Procedure

Five borders, labeled 1 through 5, were segmented using a custom-written manual segmentation procedure (MatLab, ver. 7.4; Mathworks Inc, Natick, MA), as previously reported.[14,15] The segmented borders were (1) INL/OPL: the border between the inner nuclear layer (INL) and the outer plexiform layer (OPL); (2) OLM: outer limiting membrane; (3) IS/OS: the border between the inner segment (IS) and outer segment (OS) of the receptors; (4) OS/RPE: border between the OS and the RPE; and (5) BM/choroid: the border between Bruch's membrane (BM) and the choroid. An example of this segmentation and the outer retinal layers that we analyzed for thickness measurements is shown in Figure 3.

Given the difficulties inherent in accurately determining the inner and outer limits of the outer nuclear layer (ONL),[15] we reported the thickness of the ONL+, which incorporates the receptor cell bodies, receptor Henle fibers, and OPL connection to cells of the INL.[15] Furthermore, as the resolution of SD-OCT does not allow distinction between BM and RPE, the reported RPE thickness is the sum of RPE and BM thicknesses.

Mean thicknesses of the ONL+, OS, and RPE layers were calculated over horizontal distances of 150 μm at each degree, from 12° nasal to 12° temporal to the center of the horizontal line scan. For the peripapillary region, mean thicknesses were determined from 1° to 4° temporal to the optic disc. The optic disc edge was determined from both the en face and SD-OCT images.

Fundus Autofluorescence Imaging

FAF imaging was performed with a confocal scanning laser ophthalmoscope (Spectralis HRA+OCT or HRA2; Heidelberg Engineering) after pupil dilation with topical 1% tropicamide. A standard procedure was followed for the acquisition of the images. Separate FAF images centered on the fovea and on the optic disc were acquired to characterize the macula and peripapillary retina respectively (Fig. 2). Peripapillary sparing on FAF was defined as the presence of a uniform autofluorescence pattern in this region (Figs. 4A, 4B). Loss of sparing was characterized by the presence of hyperautofluorescent flecks or any pattern of hypoautofluorescence (i.e., RPE atrophy [Fig. 4C]) in the peripapillary retina, typical of *ABCA4* retinopathy. SD-OCT images in Figures 4D–F correspond to the FAF images in Figures 4A–C. The black double-headed arrows indicate regions where there was loss of IS/OS in the macula, this being most extensive in Figure 4F. The single white arrows indicate regions of peripapillary sparing (i.e., a uniform fluorescence pattern on FAF and preserved IS/OS in the peripapillary region on SD-OCT). Double white arrows indicate regions of peripapillary atrophy on FAF with a corresponding loss of IS/OS in this region on SD-OCT (Figs. 4C, 4F).

Genotyping

Screening for mutations in the *ABCA4* gene was performed using the ABCR500 microarray, which detects all known mutations in the *ABCA4* gene. Mutations were confirmed by direct sequencing.[16,17] A selection of patients who had one mutation detected by these conventional methods had complete sequencing of the *ABCA4* gene performed using next-generation sequencing (454 platform; Roche Diagnostics, Indianapolis, IN).[18]

Statistical Analysis

The 95% CI was used to determine the significance of thickness changes between controls and individual patients. Correlations between the thickness of the retinal layers and visual sensitivities were calculated using linear regression after conversion of TDs to log values and then to a linear scale. One-way analysis of variance (ANOVA) was used to assess the significance of detected differences between the nasal and temporal macular thicknesses in controls and patients (SPSS, ver. 15.00; SPSS, Inc., Chicago, IL). Tukey-Kramer post hoc analysis was also performed to further assess between-group differences. $P < 0.05$ was considered statistically significant.

RESULTS

Demographic, genetic, and clinical information for all the patients is summarized in Table 1. All 27 patients (from 25

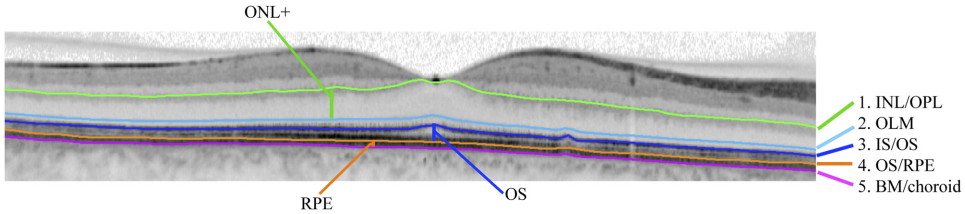

FIGURE 3. An example of a segmented SD-OCT scan through the fovea is presented. The ONL+ (from OLM to INL/OPL), OS (from OS/RPE to IS/OS), and RPE (from BM/choroid to OS/RPE) layers are demonstrated.

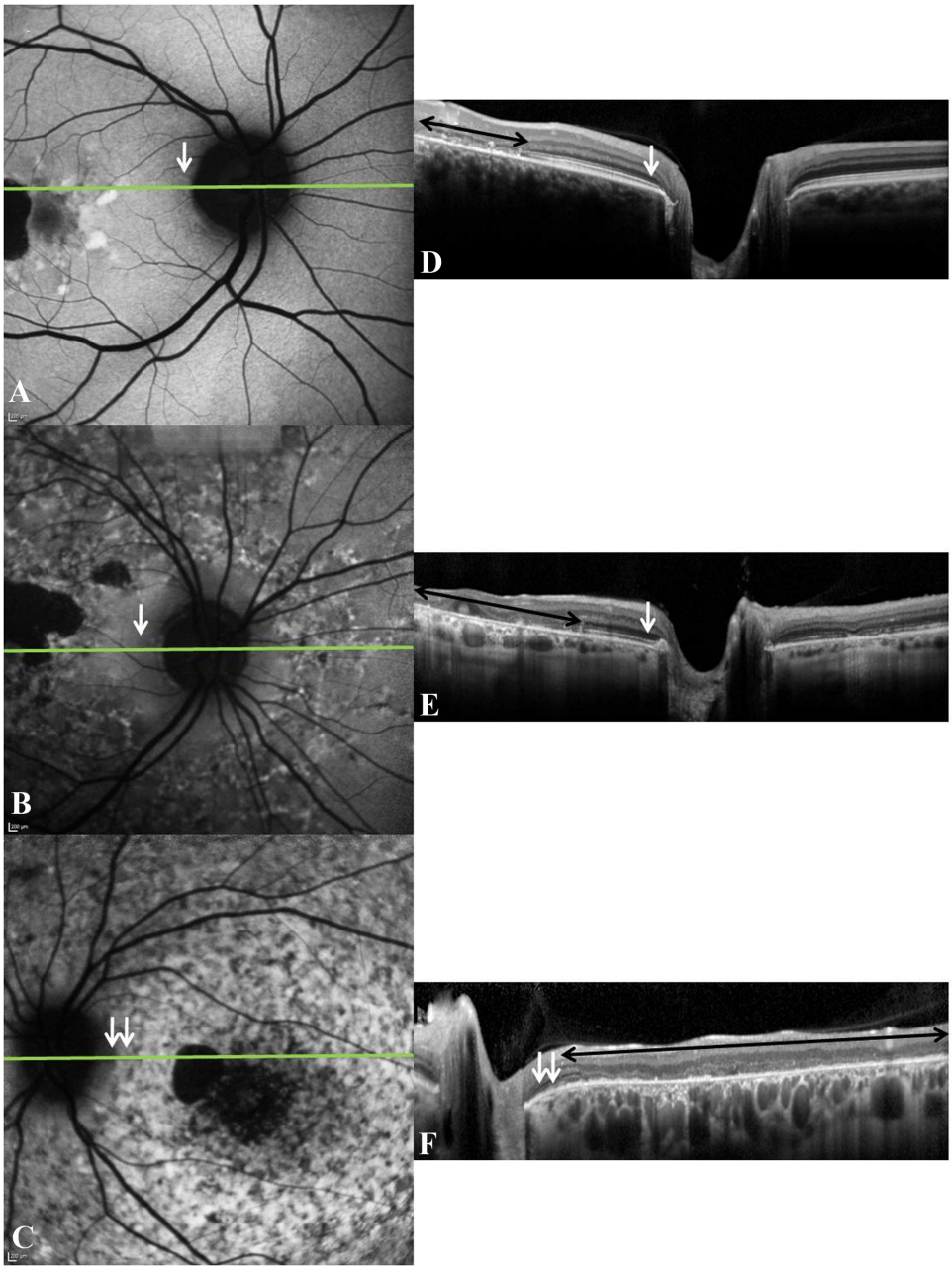

FIGURE 4. (**A**–**C**) The various patterns of peripapillary autofluorescence in STGD1; (**D**–**F**) the corresponding SD-OCT line scans (position indicated on FAF image by the *horizontal green line*). Peripapillary sparing (*white arrows*) is seen in (**A**) and (**D**) and (**B**) and (**E**). Peripapillary atrophy (*double white arrows*) is seen in (**C**) and (**F**). *Black double-headed arrows*: regions where there was loss of IS/OS in the macula.

families) had at least one mutation detected in the *ABCA4* gene, with both mutations detected in 20 patients. One patient had three mutations detected in the *ABCA4* gene; however, segregation analysis was not performed because of the unavailability of parental DNA. Twenty-two patients had ERG group I and 5 had ERG group II disease. Based on FAF, 13 patients had disease that extended outside the macula. Although five patients had FAF abnormalities in the peripapillary area, only two had peripapillary hypoautofluorescence, which was patchy, surrounding the optic disc. The other three patients demonstrated peripapillary hyperautofluorescent flecks in various distributions.

The eccentric PRL ranged from 1° to 14° superior to the fovea in 19 patients with ERG group I disease and from 1° to 10° superior to the fovea in 4 patients with ERG group II disease. The remaining four patients, with foveal PRL, had evidence of relative foveal sparing on FAF and SD-OCT (Table 1).

Macular SD-OCT

Figure 5 presents the mean thicknesses of the ONL+, OS, and RPE layers measured from 12° nasal to 12° temporal to the fovea. The columns show the results for the mean of the two ERG groups ±1 SE (solid red and dashed green lines), each compared with the mean ±1 SE for the age-similar controls (solid black and dashed blue lines). The eccentricities 9° from the fovea in the nasal (−) and temporal (+) macula are indicated by the black vertical dashed lines. Preservation of structure beyond 9° was suggested by mean thicknesses that were equal to or greater than those of the control group (black arrow). In the patients with ERG group I disease, the mean thickness of the ONL+ was preserved in the nasal macula, whereas the mean OS layer thickness showed preservation in both the nasal and temporal macula. On the other hand, in the patients with ERG group II disease, only the mean OS layer thickness in the nasal macula showed evidence of preserva-

Table 1. Summary of Clinical, Demographic, and Genetic Data

Patient	Sex	Age at Exam (y)	Eye	VA	BCEA 1 SD (deg^2)	Eccentricity of PRL (deg)	ERG Group	FAF Abnormalities		Allele 1	Allele 2	Allele 3
								Distribution	Peripapillary Area			
1	F	43	OS	20/20	0.73	0	II	M	—	A1799D	ND	ND
2	M	30	OS	20/150	3.21	6	I	M	—	T1253M	G1961E	ND
3	F	55	OD	20/30	1.82	0	I	EM	—	G863A	IVS28+5 G>T	ND
4	M	44	OD	20/25	0.65	0	I	M	—	E161K	ND	ND
5.1	F	24	OD	20/200	1.57	1	I	M	—	L541P/A1038V	G1961E	ND
5.2	F	22	OD	20/30	2.74	1	I	M	—	L541P/A1038V	G1961E	ND
6.1	F	21	OD	20/150	2.01	1	I	M	—	L541P/A1038V	G1961E	ND
6.2	F	18	OS	20/100	3.09	4	I	M	—	L541P/A1038V	G1961E	ND
7	F	27	OS	20/400	2.97	9*	II	EM	Peripapillary atrophy	L2027F	G851D	ND
8	M	34	OS	20/100	2.16	4	I	M	—	G1961E	G1961E	ND
9	M	20	OS	20/150	2.77	4	I	M	—	IVS20+5 G>A	G1961E	ND
10	F	23	OS	20/150	9.05	5	I	M	—	L541P/A1038V	I1846T	ND
11	M	59	OS	20/100	6.52	10	II	EM	—	P1380L	S1696N	ND
12	M	49	OD	20/150	9.97	1	I	EM	Nasal+temporal flecks	R1108H	P1380L	ND
13	M	47	OS	20/80	5.62	7	I	EM	—	G863A	Y106X	ND
14	F	42	OD	20/200	9.53	9	I	EM	Temporal flecks	N965S	ND	ND
15	M	14	OD	20/200	23.84	1	II	EM	Nasal flecks	IVS38-10 T>C	IVS40+5 G>A	ND
16	M	52	OS	20/20	1.3	0	I	M	—	IVS38-10 T>C	ND	ND
17	M	34	OS	20/30	2.8	1	I	M	—	L541P/A1038V	G1961E	ND
18	F	33	OD	20/100	6	6	I	M	—	G1961E	R2077W	ND
19	F	22	OS	20/60	11	4	I	M	—	A854T	A1038V	C2150Y
20	F	34	OS	20/200	14.2	14	I	EM	—	G1961E	ND	ND
21	F	19	OD	20/200	3.7	12	I	EM	—	R602W	M18821	ND
22	F	27	OD	20/400	9.6	9	II	EM	Peripapillary atrophy	P1380L	P1380L	ND
23	F	18	OS	20/50	4.9	5	I	EM	—	R1640W	V1693I	ND
24	M	22	OS	20/150	10.5	2	I	EM	—	C54Y	ND	ND
25	M	44	OS	20/150	9.1	5	I	EM	—	R1640W	ND	ND

VA, visual acuity; Rel. Unstable, relatively unstable fixation; FAF Abn, fundus autofluorescence abnormalities; M, macular only; EM, extramacular; N, nasal; T, temporal; ND, not detected.
* Nasal to fovea.

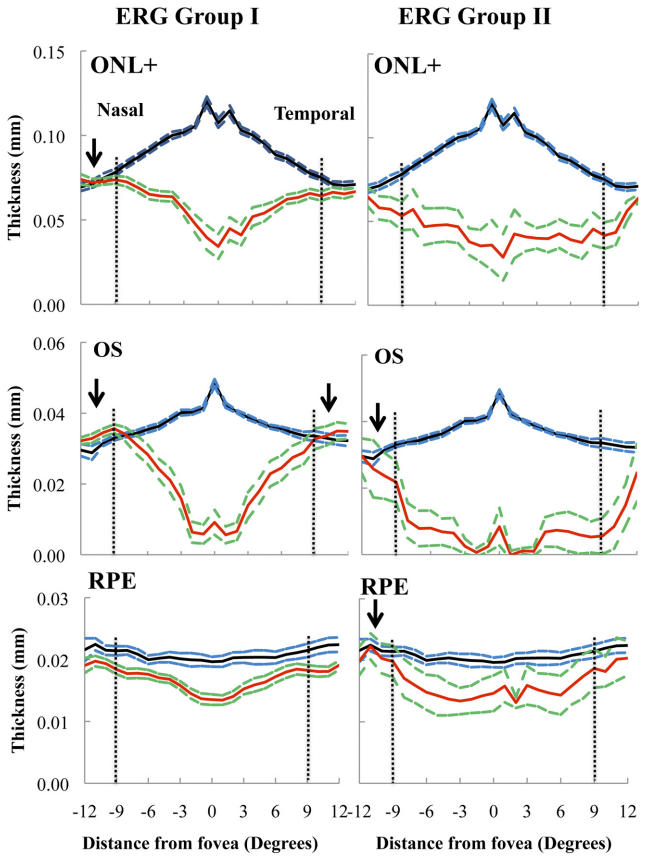

FIGURE 5. Thicknesses of the ONL+, OS, and RPE layers across the macula in patients with ERG group I or II disease. *Solid black* and *dashed blue lines*: mean thickness ±1 SE for the 12 controls. *Solid red lines*: mean values for the patients with ERG groups I and II disease; *green dashed lines*: ±1 SE for both groups. *Vertical dashed horizontal lines*: an eccentricity of 9° in the nasal (−) and temporal (+) macula. *Arrows*: regions where the mean thickness is equal to or greater than that of controls in the nasal or temporal macula.

tion. The mean RPE layer thickness demonstrated preservation in the nasal macula in the patients with ERG group II disease.

Peripapillary SD-OCT

To more specifically characterize thicknesses in the nasal macula (i.e., peripapillary area), we examined a region from 1° to 4° temporal to the optic disc edge with an SD-OCT horizontal line scan that bisected the optic disc. Acquisition of an additional horizontal line scan centered on the optic nerve was necessary for 11 controls and 24 patients for this analysis. These data were not available for two patients. Both of these siblings had disease localized to the fovea and parafovea on FAF. The results for 20 patients with ERG group I and 5 with ERG group II disease were compared with the mean ± 95% CI of the 12 controls (Fig. 6). Eight patients demonstrated thinning of the ONL+ in the peripapillary region, although thinning was not detected in four of those with ERG group I disease until an eccentricity of at least 3° from the optic disc edge was reached. OS layer thinning was detected in nine patients. A 10th patient who had ERG group I disease was borderline for significant thinning of the OS layer at 4° from the disc edge. There was marked ONL+ and OS layer thinning across the entire peripapillary area in two patients, both with ERG group II disease. They were the only patients to demonstrate peripapillary hypoautofluorescence on FAF in this study, although their RPE layer thicknesses were within normal limits in the examined temporal peripapillary area. In fact, thinning of the RPE layer in the peripapillary area was detected in only two patients: one with ERG group I and one with group II disease. Both patients had FAF abnormalities that extended outside the macula on FAF.

Nasal versus Temporal Macula

To determine whether the relative sparing of the ONL+ and OS layer thicknesses in the peripapillary macula was a function of eccentricity alone, we subtracted the mean thicknesses of these layers in the temporal macular region, from 9° to 12°, in each of the 27 patients from the mean thicknesses in an equivalent nasal region. The differences in each patient were compared to those in the controls. Relative sparing was suggested by a difference between nasal and temporal macular thickness that was greater than the maximum range detected in the controls. The data are presented in Figure 7, where the top and bottom panels present the data for the ONL+ and OS layers, respectively, of the 22 patients with ERG group I disease, the 5 patients with group II disease, and the 12 controls. In addition, we calculated the median and first and third quartile values for each group. These are presented in the same figure in the form of box-and-whisker plots, where the whiskers represent the minimum and maximum values and the thick horizontal bars represent the medians.

For the ONL+, the data showed a trend toward greater thickness in the nasal compared with temporal macula in the control group, as well as in both ERG groups. The median differences were greater in both patient groups. Importantly, in seven patients, the differences demonstrated peripapillary

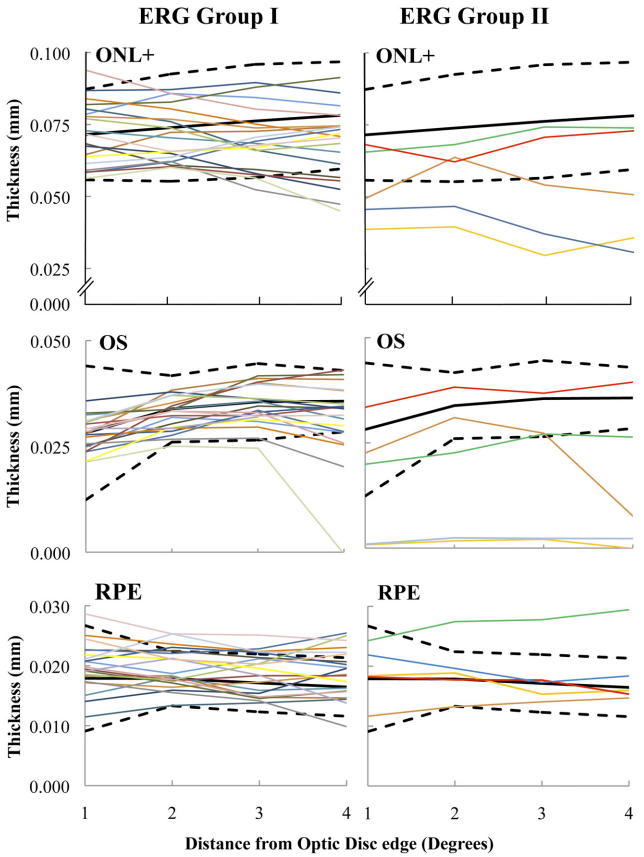

FIGURE 6. Peripapillary ONL+, OS, and RPE layer thicknesses in 20 patients with ERG group I and 5 patients with ERG group II disease (*colored lines*). *Black lines*: the mean ± 95% CI of the controls (*solid*, mean; *dashed*, CI).

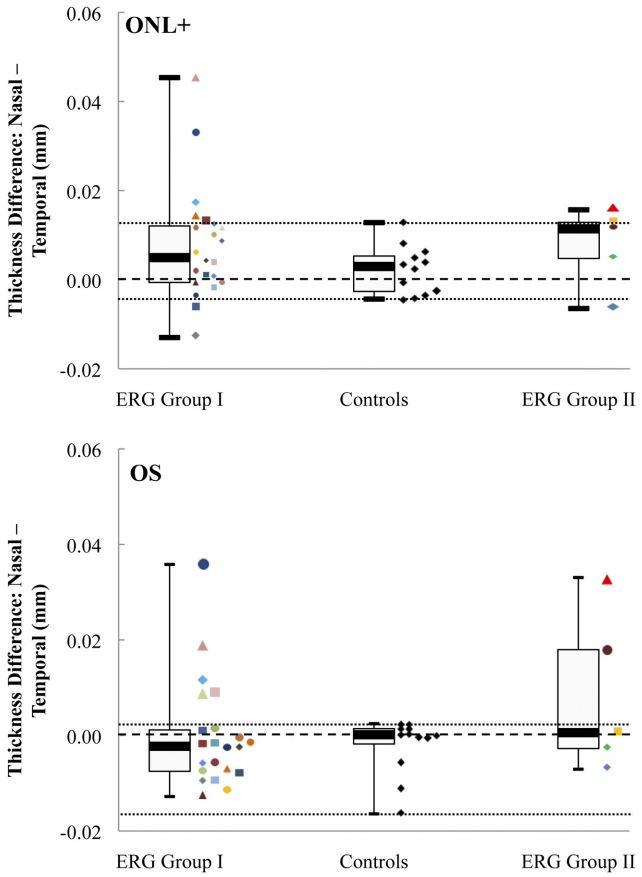

Figure 7. Box-and-whisker plots of the ONL+ and OS layer mean thicknesses differences between the nasal and temporal macula, at eccentricities from 9° to 12°, in the controls and in both ERG groups. The median values of each subgroup are presented together, with the first and third quartiles and the minimum and maximum values. *Colored symbols*: individual patient mean thickness differences values at these eccentricities. *Central black dashed line*: 0 difference; *top* and *bottom dashed lines*: the highest and lowest differences detected between the nasal and temporal macula, respectively, in the controls.

sparing that was greater than the maximum value for the controls, suggesting relative sparing of the ONL+ in the nasal region of the macula in STGD1. Five of these patients had ERG group I disease and two had ERG group II disease. Three of the five patients with ERG group I and both patients with ERG group II disease had extramacular disease on FAF. Three patients, two with ERG group I and one with ERG group II disease, had greater relative sparing of the ONL+ in the temporal macula. Two of these patients, one from each ERG group, had extramacular disease on FAF.

In the OS layer, seven patients, five with ERG group I and two with ERG group II disease, had relative peripapillary sparing (i.e., their differences were greater than the maximum value for the controls). All seven patients had FAF abnormalities that extended outside the macula.

Of the 10 patients who met our definition of relative peripapillary sparing of the ONL+ and/or OS layers, 8 had FAF abnormalities that extended outside the macula. The other two patients, both with FAF abnormalities confined to the macula and ERG group I disease, demonstrated a difference between nasal and temporal macular thicknesses in the ONL+ that was only marginally greater than the maximum values detected between the controls, whereas no such difference was found in the OS layer of either patient.

Fourteen patients had similar nasal and temporal macular thicknesses in the ONL+ and OS layers. Eleven of these had FAF abnormalities confined to the macula, 10 with ERG group I and 1 with ERG group II disease. The other three patients, all with ERG group I disease, had FAF abnormalities that extended outside the macula.

Given the evidence of relative peripapillary sparing in most of the patients with extramacular disease, we subdivided the subjects into the following three groups for statistical comparison of mean nasal with temporal ONL+ and OS layer thicknesses: controls, patients with only macular disease on FAF, and patients with extramacular disease on FAF. The within-group data analyses are presented in Table 2. In the controls no significant difference in either ONL+ or OS layer thicknesses were detected between the mean nasal and temporal macular measurements. In the patients with extramacular disease, the ONL+ thickness was significantly greater in the nasal compared with the temporal macula ($P = 0.046$), whereas in the patients with macular disease, the OS layer thickness was significantly greater in the temporal compared with the nasal macula ($P = 0.036$).

Significant between-group differences were detected for the ONL+ thicknesses in the nasal ($P = 0.019$) and temporal ($P < 0.001$) macula, as well as in the OS layer in the temporal macula ($P = 0.001$). Post hoc analysis using Tukey's honestly significant difference (HSD) test indicated that there was no significant difference in the mean nasal or temporal macular thicknesses in the controls compared with the patients with macular disease only. However the mean temporal macular thicknesses of the ONL+ and OS layers in the patients with extramacular disease were significantly thinned compared with that in the controls ($P < 0.001$ for ONL+, $P = 0.024$ for the OS layer). This result suggests the presence of relative peripapillary sparing in the patients with extramacular disease.

Microperimetry versus SD-OCT

Given our finding of relative peripapillary sparing in the patients with extramacular disease, we compared the thicknesses of the ONL+ and OS layers in the nasal and temporal macula to visual sensitivity in the patients with extramacular disease and in the patients with macular disease. We calculated the mean TDs, at eccentricities 7° and 9° from the fovea in each patient, by subtracting the visual sensitivities at these locations from those in the controls. The histograms in Figure 8 illustrate the comparison between the mean TDs (Fig. 8A) and the thicknesses of the ONL+ (Fig. 8B) and OS layers (Fig. 8C) at eccentricities 7° and 9° from the fovea in the nasal and temporal macula. In the patients with macular disease only, mean sensitivity was decreased by approximately the same amount (−2.2 and −3.2 dB, respectively) in the nasal and temporal macula. A similar pattern can be seen for the ONL+ and OS

Table 2. Comparison of Nasal and Temporal Macular Thicknesses

	Mean Nasal (SD)	Mean Temporal (SD)	*P*
ONL+			
Controls	0.074 (0.007)	0.072 (0.006)	0.361
Macular disease only	0.075 (0.009)	0.071 (0.008)	0.181
Extramacular disease	0.065 (0.013)	0.054 (0.014)	**0.046**
OS layer			
Controls	0.031 (0.003)	0.033 (0.005)	0.176
Macular disease only	0.034 (0.005)	0.038 (0.006)	**0.036**
Extramacular disease	0.029 (0.012)	0.022 (0.016)	0.337

Data are the mean (SD). Bold text highlights statistical significance ($P < 0.05$).

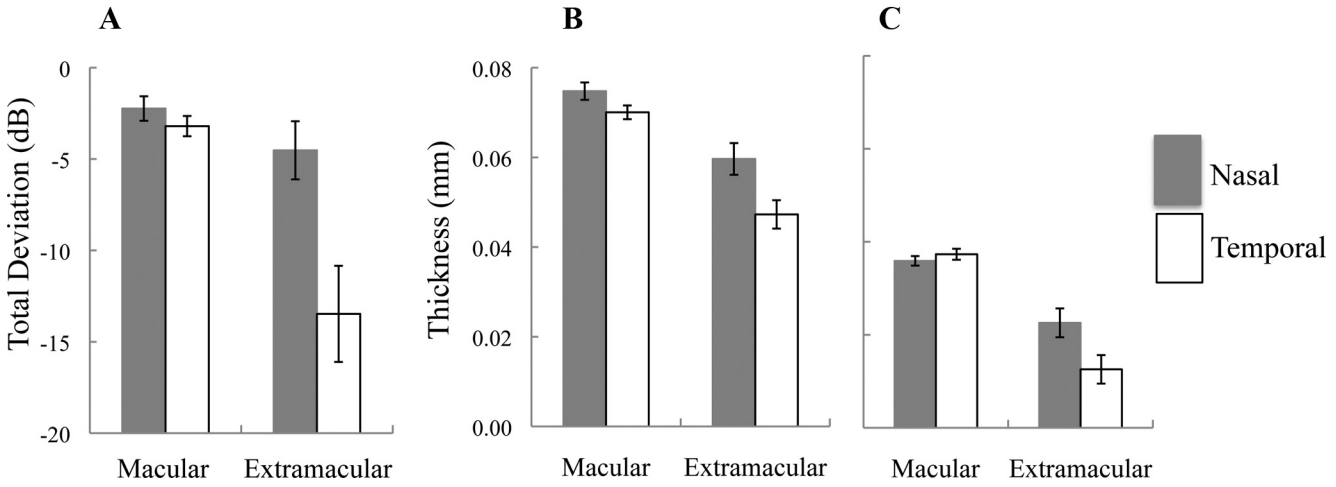

FIGURE 8. The mean TD (**A**), from 7° and 9° from the fovea, in the nasal and temporal macula in patients with macular disease only and in those with extramacular disease. Error bars, mean ± 1 SE. Data are also shown for the mean ONL+ (**B**) and OS layer (**C**) thicknesses in these subgroups, at the same eccentricities.

layer thickness values. These results contrast with the data from the patients with extramacular disease, where the temporal macular TD values and ONL+ and OS layer thicknesses, revealed greater abnormalities compared with the nasal (i.e., peripapillary) macula. Patients with extramacular disease showed a trend toward relative functional sparing in the peripapillary macula in addition to structural sparing.

Whereas visual sensitivities across the region assessed by the horizontal line scan were decreased in the central macular area, outside this central area sensitivities were less affected. A comparison of TDs (in linear units) with normalized ONL+ and OS layer thicknesses across the macula showed a higher correlation with the OS layer ($r^2 = 0.39$) compared with ONL+ thickness ($r^2 = 0.24$).

Relationship of ONL+, OS, and RPE Layer Thicknesses

To gain some insight into the sequence of events in the development of retinal and RPE atrophy in STGD1, we examined the horizontal SD-OCT line scans for the presence of significant thinning of the ONL+ and OS layers across the macula in individual patients relative to controls (mean ± 95% CI). A greater horizontal extent of significant thinning of the ONL+ compared to the OS layer was detected in 16 patients, all with ERG group I disease. Twelve of the patients had macular disease only, and four patients had extramacular disease on FAF. In contrast, only seven patients demonstrated a greater horizontal extent of significant thinning of the OS layer compared with the ONL+. Four of these patients had ERG group I and three had ERG group II disease. In three patients, a greater horizontal extent of significant thinning of either layer could not be accurately determined because of the extent of disease and the size of the area scanned. In one other patient, these extents were found to be equal.

To study the relationship between RPE and photoreceptor thickness at the earliest disease stage in STGD1, we examined patients with macular disease only. Twelve of these 14 patients had significant thinning of the RPE detected at some point along the horizontal SD-OCT line scan. When we compared the thicknesses of the RPE to those of the ONL+ and OS layers, we found significant thinning of the ONL+ and OS layers in all 14 patients at some point within regions of normal RPE thickness. Furthermore, in regions of qualitatively uniform FAF in the macula, 12 patients had significant thinning of the ONL+, and 6 had thinning of the OS layer detected.

DISCUSSION

Peripapillary sparing is a feature of *ABCA4* disease. The purpose of this study was to perform a detailed analysis of the ONL+, OS, and RPE thicknesses in this region and across the macula and to compare these results with visual function. Comparison of the nasal and temporal macular regions between 9° and 12° from the fovea suggested a trend toward preferential preservation of the ONL+ and/or OS layers in the peripapillary region in certain patients with STGD1. A detailed analysis of individual cases showed that there was relative peripapillary sparing in most of the patients who had FAF abnormalities that extended outside the macula (i.e., in the patients with more widespread disease). The ONL+ and OS layer thicknesses in these patients were greater in the nasal than in the temporal macula, and the mean temporal macular thicknesses were significantly thinned compared with those of the controls. A corresponding trend toward functional peripapillary sparing was also detected in these patients. However, in the patients with ERG group I disease who had FAF abnormalities confined to the central macula, nasal and temporal macular thicknesses tended to be equivalent. With regard to the RPE, the mean thicknesses were reduced across the entire macula, although a greater trend toward normal mean thickness was observed in the nasal and temporal macula with ERG group II disease.

Only two patients showed significant thinning of the ONL+ and OS layers across the entire peripapillary region on the horizontal line scans bisecting the optic nerve; these patients demonstrated abnormalities on FAF surrounding the optic disc, as well as having ERG group II disease. Importantly, only two patients had thinning of the RPE detected in the peripapillary region, one from each ERG group. These changes were not associated with peripapillary hypoautofluorescence on FAF.

The results of this study are in keeping with the histopathologic results of an eye of a patient with a clinical diagnosis of STGD1, which demonstrated disorganization of photoreceptors from eccentricities of 0.7 mm from the optic disc edge,[19] (i.e., between 2° and 3°). A corresponding eccentricity of 0.6 mm has been reported as the outer boundary of the relatively spared peripapillary region, based on FAF findings.[2]

The reasons for this relative sparing in the presence of widespread disease remain unclear. A more favorable photoreceptor:RPE ratio in the peripapillary area has been suggested, as well as less photo-oxidative damage or lipofuscin buildup

due to a reduced light load on the photoreceptor–RPE complex in the presence of a thicker overlying peripapillary retinal nerve fiber layer (RNFL).[2] Loss of peripapillary sparing may well be mutation dependent, in that the more severe the mutation in the *ABCA4* gene, the more likely the development of peripapillary atrophy. The adaptive optics scanning laser ophthalmoscope has recently been used to demonstrate normal cone spacing in the temporal peripapillary retina of patients with STGD1 in comparison to other abnormal macular regions.[20]

We know from the natural history of STGD1 that the disease process, in general, moves centrifugally. Despite the limitation of the cross-sectional design of our study, on the basis of our findings that for most of the patients there was significant thinning of the ONL+ in regions of normal OS thickness, we propose that thinning of the ONL+ may precede OS layer thinning in STGD1. Thinning of the ONL has been recently reported in the $Abcr^{-/-}$ mouse, the animal model for STGD1, and this has been suggested as a possible marker for monitoring treatment effect in preclinical trials in animal models.[21] As such, measurement of the ONL+ and OS layers obtained using SD-OCT may provide a useful quantitative parameter for monitoring disease progression and treatment effect in humans.

The exact sequence of events in the development of atrophy in STGD1 remains controversial. Although it is generally accepted that atrophy of the RPE occurs initially, with secondary photoreceptor degeneration, Gomes et al.[22] reported disorganization of the photoreceptors in regions of relatively preserved RPE based on SD-OCT and FAF findings. This suggests that degeneration of the photoreceptors may occur before that of the RPE. We found significant thinning of the ONL+ and OS layers in regions where RPE layer thickness and FAF were normal, although the RPE layer thicknesses were at the lower end of normal. These results support the theory that changes in the photoreceptor layer may occur before the development of abnormalities in the RPE layer.

Our study has some limitations. First, extramacular disease, based on FAF findings, was detected in only 13 of the 27 patients. Given that we excluded patients with ERG group III disease due to eccentricity and instability of fixation, the proportion of STGD1 patients with FAF abnormalities extending outside the macula is likely to be higher than that reported in this study,[8] and so our results may have underestimated the degree of peripapillary involvement by excluding these more severely affected patients. Second, the number of patients with ERG group II disease was small, and so it is important to be cognizant of the results of the individual patients within this group when discussing results in aggregate. However, group II is the least commonly detected of the three ERG groups.[8,9] Third, the RPE thickness was reported together with that of BM, and so we must exercise caution in attributing significance to thickness changes in this reported layer. Although we know that there is an age-dependent increase in the thickness of BM,[23] histopathologic data on BM thickness in *ABCA4* disease was not available in the literature. Importantly, there was no significant difference in the age profile of the patients and controls in this study. Finally, the presence of a superior PRL in STGD1 meant that the microperimetry data in the nasal and temporal macula were not available for all patients, and there were fewer test points to compare, thus reducing the amount of functional data that could be compared with structural data in assessing peripapillary sparing.

Although recent studies have shown variable effects of mutations in the *ABCA4* gene on the RNFL thickness using SD-OCT,[24,25] to our knowledge, this study is the first report of the use of SD-OCT and microperimetry to demonstrate relative sparing of peripapillary outer retinal structure and function in STGD1. Understanding this complex relationship may provide further avenues for monitoring disease progression and treatment effect in the future.[26] Furthermore, our results support the hypothesis that photoreceptor degeneration may occur earlier than RPE degeneration in STGD1.

References

1. Allikmets R, Singh N, Sun H, et al. A photoreceptor cell-specific ATP-binding transporter gene (ABCR) is mutated in recessive Stargardt's macular dystrophy. *Nat Genet.* 1997;15:236–246.
2. Cideciyan AV, Sider M, Aleman TS et al. ABCA4-associated retinal degenerations spare structure and function of the human parapapillary retina. *Invest Ophthalmol Vis Sci.* 2005;46:4739–4746.
3. Schwoerer J, Secrétan M, Zografos L, Piguet B. Indocyanine green angiography in fundus flavimaculatus. *Ophthalmologica.* 2000; 214:240–245.
4. Klein R, Lewis RA, Meyers SM, Myers FL. Subretinal neovascularization associated with fundus flavimaculatus. *Arch Ophthalmol.* 1978;96:2054–2057.
5. Lois N, Halfyard AS, Bird AC, Holder GE, Fitzke FW. Fundus autofluorescence in Stargardt macular dystrophy-fundus flavimaculatus. *Am J Ophthalmol.* 2004;138:55–63.
6. Hwang JC, Zernant J, Allikmets R, et al. Peripapillary atrophy in Stargardt disease. *Retina.* 2009;29:181–186.
7. Jayasundera T, Rhoades W, Branham K, et al. Peripapillary dark choroid ring as a helpful diagnostic sign in advanced Stargardt disease. *Am J Ophthalmol.* 2010;149:656–660.
8. Burke TR, Allikmets R, Smith RT, et al. Loss of peripapillary sparing in non-group I Stargardt disease. *Exp Eye Res.* 2010;91:592–600.
9. Lois N, Holder GE, Bunce E, et al. Phenotypic subtypes of Stargardt macular dystrophy-fundus flavimaculatus. *Arch Ophthalmol.* 2001; 119:359–369.
10. Timberlake GT, Mainster MA, Peli E, et al. Reading with a macular scotoma, 1: retinal location of scotoma and fixation area. *Invest Ophthalmol Vis Sci.* 1986;27:1137–1147.
11. Marmor MF, Holder GE, Seeliger MW, Yamamoto S. International Society for Clinical Electrophysiology of Vision: standard for clinical electroretinography (2004 update). *Doc Ophthalmol.* 2004; 108:107–114.
12. Rohrschneider K. Determination of the location of the fovea on the fundus. *Invest Ophthalmol Vis Sci.* 2004;45:3257–3258.
13. Timberlake GT, Sharma MK, Grose SA, et al. Retinal location of the preferred retinal locus relative to the fovea in scanning laser ophthalmoscope images. *Optom Vis Sci.* 2005;82:177–185.
14. Hood DC, Lin CE, Lazow MA, Locke KG, Zhang X, Birch DG. Thickness of receptor and post-receptor retinal layers in patients with retinitis pigmentosa measured with frequency-domain optical coherence tomography. *Invest Ophthalmol Vis Sci.* 2009;50: 2328–2336.
15. Hood DC, Lazow MA, Locke KG, Greenstein VC, Birch DG. The transition zone between healthy and diseased retina in patients with retinitis pigmentosa (RP). *Invest Ophthalmol Vis Sci.* 2011; 52:101–108.
16. Jaakson K, Zernant J, Külm M et al. Genotyping microarray (gene chip) for the ABCR (ABCA4) gene. *Hum Mutat.* 2003;22:395–403.
17. Klevering BJ, Yzer S, Rohrschneider K et al. Microarray-based mutation analysis of the ABCA4 (ABCR) gene in autosomal recessive con-rod dystrophy and retinitis pigmentosa. *Eur J Hum Genet.* 2004;12:1024–1032.
18. Meyer M, Stenzel U, Hofreiter M. Parallel tagged sequencing on the 454 platform. *Nat Protoc.* 2008;3:267–278.
19. Birnbach CD, Jarvelainen M, Possin DE, Milam AH. Histopathology and immunocytochemistry of the neurosensory retina in fundus flavimaculatus. *Ophthalmology.* 1994;101:1211–1219.
20. Chen Y, Rathnam L, Sundquist SM, et al. Cone photoreceptor abnormalities correlate with vision loss in patients with Stargardt disease. *Invest Ophthalmol Vis Sci.* 2011;52:3281–3292.

21. Wu L, Nagasaki T, Sparrow J. R. Photoreceptor cell degeneration in Abcr$^{-/-}$ Mice. *Adv Exp Med Biol.* 2010;664:533–539.
22. Gomes N, Greenstein VC, Carlson JN, et al. A comparison of fundus autofluorescence and retinal structure in patients with Stargardt disease. *Invest Ophthalmol Vis Sci.* 2009;50:3953–3959.
23. Killingsworth MC. Age-related components of Bruch's membrane in the human eye. *Graefes Arch Clin Exp Ophthalmol.* 1987;225:406–412.
24. Pasadhika S, Fishman GA, Allikmets R, Stone EM. Peripapillary retinal nerve fiber layer thinning in patients with autosomal recessive cone-rod dystrophy. *Am J Ophthalmol.* 2009;148:260–265.
25. Genead MA, Fishman GA, Anastasakis A. Spectral-domain OCT peripapillary retinal nerve fibre layer thickness measurements in patients with Stargardt disease. *Br J Ophthalmol.* 2010;95:689–693.
26. Charbel Issa P, Troeger E, Finger R, et al. Structure-function correlation of the human central retina. *PloS One.* 2010;5:e12864.